



## LJMU Research Online

**Fang, S, Liu, Z, Wang, X, Wang, J and Yang, Z**

**Simulation of evacuation in an inclined passenger vessel based on an improved social force model**

<http://researchonline.ljmu.ac.uk/id/eprint/16961/>

### Article

**Citation** (please note it is advisable to refer to the publisher's version if you intend to cite from this work)

**Fang, S, Liu, Z, Wang, X, Wang, J and Yang, Z (2022) Simulation of evacuation in an inclined passenger vessel based on an improved social force model. Safety Science, 148. p. 105675. ISSN 0925-7535**

LJMU has developed [LJMU Research Online](#) for users to access the research output of the University more effectively. Copyright © and Moral Rights for the papers on this site are retained by the individual authors and/or other copyright owners. Users may download and/or print one copy of any article(s) in LJMU Research Online to facilitate their private study or for non-commercial research. You may not engage in further distribution of the material or use it for any profit-making activities or any commercial gain.

The version presented here may differ from the published version or from the version of the record. Please see the repository URL above for details on accessing the published version and note that access may require a subscription.

For more information please contact [researchonline@ljmu.ac.uk](mailto:researchonline@ljmu.ac.uk)

<http://researchonline.ljmu.ac.uk/>



# Simulation of evacuation in an inclined passenger vessel based on an improved social force model

Siming Fang<sup>a,b</sup>, Zhengjiang Liu<sup>a,b</sup>, Xinjian Wang<sup>a,b</sup>, Jin Wang<sup>c</sup>, Zaili Yang<sup>c,d,\*</sup>

<sup>a</sup> Navigation College, Dalian Maritime University, Dalian 116026, PR China

<sup>b</sup> Key Laboratory of Navigation Safety Guarantee of Liaoning Province, Dalian 116026, PR China

<sup>c</sup> Liverpool Logistics, Offshore and Marine (LOOM) Research Institute, Liverpool John Moores University, L3 3AF, UK

<sup>d</sup> Transport Engineering College, Dalian Maritime University, Dalian 116026, PR China

## ARTICLE INFO

### Keywords:

Ship inclination  
Social force model  
Safety evacuation  
Ship safety  
Evacuation analysis  
Passenger vessel

## ABSTRACT

Passenger vessels often present different heeling and/or trim angles during and after accidents, while recognising it as the main factor affecting pedestrian movement during an emergency evacuation process, there is difficulty to reproduce the evacuation activities on ships due to cost constraints and safety concerns in relevant studies. To fill the research gap, an improved social force model (SFM) incorporating both inclining and self-adjusting forces of pedestrians into the basic SFM model was constructed to simulate the pedestrian dynamics under different ship trim and heeling circumstances. The improved SFM also includes a reduction law of pedestrian speed at different heeling and/or trim angles and adds a calculation of the reduction factor in each time step. It enables the simulation of the pedestrian movement process on inclined vessels accurately. The simulation results show that when the inclination angle is less than 20°, the impact of both heeling and/or trim on an individual's walking speed and evacuation time are weaker than the one with an angle exceeding 20°. When passengers walk along the keel line on an inclined ship, the impact of heeling on speed attenuation is more significant than the one of trim. The overall evacuation time is extended with the increasing number of evacuees. The flow rate at the exit reaches the maximum when the number of evacuees is 100, and the average evacuation rate is 2.01 persons/s. The findings provide useful insights on crowd management in the process of passenger vessel evacuation under an inclined state.

## 1. Introduction

In its rapid and large-scale development, cruise shipping has attracted increasing safety concerns from the public. Evacuation is recognised as an effective means to reduce casualties when emergencies occur during the operation of passenger vessels (Huang et al., 2021; Xie et al., 2020a; Xie et al., 2020b). However, compared with the evacuation process in other fields, ship evacuation has its own unique characteristics such as restricted evacuation environments, complex behaviours of evacuees, and special assembly areas (Wang et al., 2021c; Wang et al., 2020; Xie et al., 2020c). Therefore, the behaviour of evacuees and the overall environment of a passenger vessel should be thoroughly and comprehensively taken into account when evacuating passengers on board (Ha et al., 2012).

Apart from a few accident cases in which ships capsized instantaneously, the process of ship evacuation can last for a time span (Wang

et al., 2021a). During this period, the ship will be highly likely inclined in a dynamic manner due to collision, grounding or other causes. Then the ship inclination changes with the external environment, resulting in a dynamic motion. At this time, evacuees often show the phenomenon of walking difficulty and evacuation stagnation due to the inclination. Therefore, the analysis of evacuation process under static inclination can be used as the baseline for research against moving ships. Two typical examples are demonstrated in Fig. 1. The “Costa Concordia” (Fig. 1 (a)) and “Sewol” (Fig. 1 (b)) shipwrecks drew widespread attention, both of them resulted in heavy casualties (Bartolucci et al., 2021; Kim et al., 2016).

Often after the occurrence of an accident, the master does not have to immediately make the decision to abandon ship and notify passengers to evacuate before the assessment of the damage. Such assessment process may delay the evacuation and passengers miss the most effective evaluation time window. In light of the possible delay, it is crucial to

\* Corresponding author at: Liverpool Logistics, Offshore and Marine (LOOM) Research Institute, Liverpool John Moores University, L3 3AF, UK.  
E-mail address: [Z.Yang@ljmu.ac.uk](mailto:Z.Yang@ljmu.ac.uk) (Z. Yang).

<https://doi.org/10.1016/j.ssci.2022.105675>

Received 6 July 2021; Received in revised form 30 November 2021; Accepted 9 January 2022

Available online 21 January 2022

0925-7535/© 2022 The Authors. Published by Elsevier Ltd. This is an open access article under the CC BY license (<http://creativecommons.org/licenses/by/4.0/>).



(a) Costa Concordia disaster



(b) Sewol-ho chimmol sago

Fig. 1. Costa Concordia and Sewol disasters.

determine the time to abandon the ship and begin evacuation and improve the safety and efficiency of the evacuation process in case of an emergency. Within this context, understanding and evaluating the movement characteristics of pedestrians on an inclined vessel become necessary and beneficial. Therefore, evacuation in an inclined room is studied by simulation, aiming to find out the changes of an individual's walking speed and evacuation time with different trim and heeling angles. The results can be fed into evacuation software to extend the simulation analysis to the entire decks or even an entire ship. Furthermore, the conclusions can provide useful insights for developing effective evacuation strategies during capsizing in reality.

The rest of the paper is organized in 5 sections. In Section 2, we introduce an extended simulation model and a review of ship evacuation process in the case of inclination. It is followed by Section 3 in which the detailed description of the model extensions and calculation flow of the improved model is presented. Section 4 presents the verification of the model. In Section 5, the results of the impact of inclination on evacuation are presented. Finally, the conclusions and useful implications are summarized in Section 6.

## 2. Related works

To tackle passenger vessel safety accidents, in 2016, the International Maritime Organization (IMO) approved a new version of the "Revised Guidelines for Evacuation Analysis for New and Existing Passenger Ships" (IMO, 2016), hereinafter referred to as the "Guidelines". It provides a series of parameters and scenarios for passenger evacuation analysis and encouraged member states to carry out the relevant evacuation experiment and simulation. Therefore, it also stimulates an increasing number of research on ship evacuation, however research on model simulations of evacuation is relatively scarce. In light of the research gap, the SFM in different evacuation scenarios is thoroughly reviewed in Section 2.1, and an analysis of experimental and simulation studies on ship evacuation under inclination is presented in Section 2.2.

### 2.1. Social force model for evacuation analysis

At present, more and more numerical models are used in various simulation studies in real-life, and the most widely used evacuation models include agent-based model (ABM), the discrete model represented by cellular automata (CAM), and the continuous model represented by SFM (Helbing and Molnar, 1995). ABM refers to a distributed method for solving complex system in recent years (Clark et al., 2021). As a microscopic model of evacuation, ABM drives the simulation to run by setting the rules of agents' behaviour and the interaction rules between agents and others and environment, which can not only aid to observe the macro emerging phenomenon but also help effectively analyse the behaviour of each individual and the interaction between individuals and environments (Bao and Huo, 2021; Hwang and Heo,

2021). The CAM was initially introduced into pedestrian evacuation simulation research by Blue and Adler (1998), where time, space and state in the model are all discrete and the moving process of pedestrians is determined by a series of motion rules until successful evacuation. As a typical microscopic discrete model, CAM divides an evacuation area into several cells. In each time step, each cell is idle or occupied by pedestrians and obstacles, and pedestrians move to a neighbouring idle cell according to the motion rules (Ruggiero et al., 2018). The SFM, as a widely used microscopic continuous model, defines the movement of pedestrians as a form of force, which includes the desired force for targets, interaction force between boundaries, obstacles and other pedestrians, etc. Newton's second law of motion was used to determine the pedestrian dynamics law in a 2-dimensional or improved 3-dimensional space. At present, this model has been widely applied to various evacuation processes and can successfully recreate some self-organization phenomena seen in real-world evacuation processes, such as the "fast is slow" phenomenon (Helbing et al., 2000; Helbing and Molnar, 1995; Kang et al., 2019; Liu et al., 2018; Ma et al., 2017).

The aforementioned microscopic models (e.g. ABM and CAM) have discrete characteristics, and the speeds are defined subjectively, which influences the impact of ship inclination on an individual's speed. Therefore, the SFM is chosen as the basic model in this study to simulate the evacuation process under inclined vessels. The reasons for the SFM selection are fourfold. The first is that SFM as a classical continuous micro simulation model has been applied in many excellent simulation software (such as AnyLogic, Viswalk), and users can modify and further develop the SFM to simulate more complex and larger areas. Compared with the several fixed movement directions of pedestrians in CAM, SFM can take into account the moving direction(s) accurately, so it is suitable for describing passenger evacuation in an inclined environment to meet the needs of this study. The third reason is that SFM not only represents various collective behaviours and self-organized phenomena but also can be improved by introducing some particular physical and psychology forces in an emergency to make simulation better mirror its reality. Lastly, SFM is modelled in the form of forces rather than setting moving parameters directly, thus considering the modelling in an inclined vessel, there will be fewer variables required in SFM compared with other models. Furthermore, previous studies on SFM have provided mature selection of parameters value which provides extra assurance for the success of the associated experiments (Helbing and Molnar, 1995; Kang et al., 2019; Ma et al., 2019).

Human behaviour is an important part of pedestrian movement simulation models. In an initial SFM, only the basic relevant forces were considered, which can simulate the process of evacuation under normal circumstances. However, researchers modified the basic SFM for different scenarios of emergency evacuation. Zhang et al. (2018) developed an improved two-layer SFM to reflect the process of pedestrian group gathering more realistically during earthquake evacuation. Ma et al. (2017; 2016) considered that the smoke generated by fire

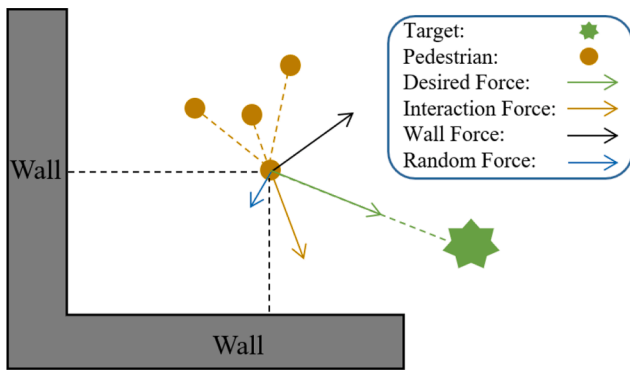


Fig. 2. Schematic diagram of the social force model.

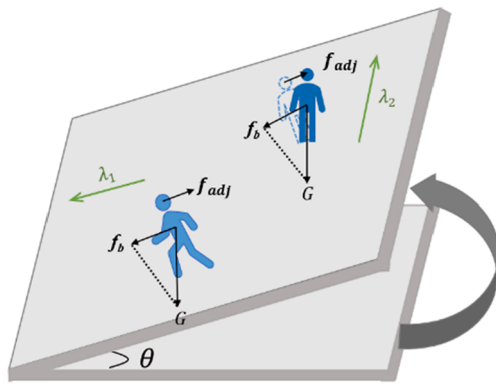


Fig. 3. The relationship between the inclination direction and moving direction.

would reduce the visibility of pedestrians and leaders were added to the SFM under restricted visibility. Johansson et al. (2015) developed an improved pedestrian waiting behaviour model based on the initial SFM, that is, three kinds of waiting models for pedestrian decision-making were created. Li et al. (2021) proposed an improved model based on a height map, which could better reproduce the temporal-spatial behaviour of evacuees on stairs, to understand the effect of stairs in a building on the evacuation process during an emergency evacuation. Liu et al. (2018) used a video data-driven technology to precisely restore the pedestrian position during an actual evacuation process, extracted the motion trajectory of pedestrians and defined the fitness function for pedestrian target selection. At the same time, by quantifying the numerical relationship between pedestrians, the “group force” was added to the SFM, an improved SFM based on video data was established. Liang et al. (2020) focused on the merging behaviour in a Y-shaped channel and added a centripetal force to the SFM to simulate the evacuation process of pedestrians in a Y-shaped passage area.

It is evident that improved SFMs are mainly used in the field of land-based evacuation; few studies in the existing literature consider the characteristics of ship passenger evacuation. Compared with the characteristics of land-based evacuation, passengers being presented in the living areas on ships face a more dynamic evacuation scenario, in which unique features of the ship environment (e.g. inclination, ship motion, particular layout) have to be incorporated during an emergency. When a ship encounters an accident such as collision, flooding, or grounding, it very likely involves a state of inclination. If the listing continues to worsen, the ship might eventually capsize. Therefore, it is crucial and beneficial to analyse ship evacuation under inclination in emergencies and reduce the loss caused by accidents. In addition, SFM is a distributed method for solving complex systems, it is often used in the case that the evacuation surface is flat and the evacuation surface has a slope in recent years. After this improvement, it can meet the evacuation requirements of inclined ships.

### 2.2. Study on passenger ship evacuation

To study the walking characteristics of pedestrians in inclined vessels, researchers have carried out relevant experiments and simulations. Sun et al. (2018a; 2018b) designed a corridor simulator to study the influence of different inclination angles on pedestrians’ walking speed. It revealed that the average individual walking speed was greatly reduced by considering the heeling and/or trim angles. Compared with the trim on a ship, the heeling angle had a less influence on the speed. Kim et al. (2019) used a truck bucket as experimental equipment to reproduce a scene similar to the inclination of a ship and measured the walking speed of pedestrians in various postures. It was also found that the density of the surrounding people would slow down the normal walking speed of passengers. Lee et al. (2004) built a ship corridor platform to simulate inclined scenarios with trim angles from  $-20^\circ$  to  $20^\circ$  and heeling angles from  $0^\circ$  to  $20^\circ$ , and studied the walking speed reduction of a single individual and a group on the platform. Bles et al. (2001) constructed a ship motion simulator installed on a hydraulic device to determine the effect of inclination or motion on the walking speed of people on corridors and staircases on ships. Katsuhara et al. (1999; 1997) conducted a full-scale trial evacuation experiment of 356 students and teachers and 27 crew members on a ferry, recorded the walking speed of participants during the inclining and rolling of the ship, and carried out simulations under the same experimental conditions. Finally, the full-scale results and simulation were compared. Wang et al. (2021b) collected the normal walking and fast walking speeds of individuals during ship berthing and encountered a small angle of rolling during ship operation. Under the same rolling angle, the higher the deck on which the pedestrians walk, the greater the reduction of the walking speed is. Considering cost and safety issues, most of the experimental scenarios were based on simulated corridors, and rarely conducted in large spaces/rooms. Nevertheless, the previous experimental results can be used as references, to help calibrate our simulation results. By comparing these findings, errors in simulation can be avoided

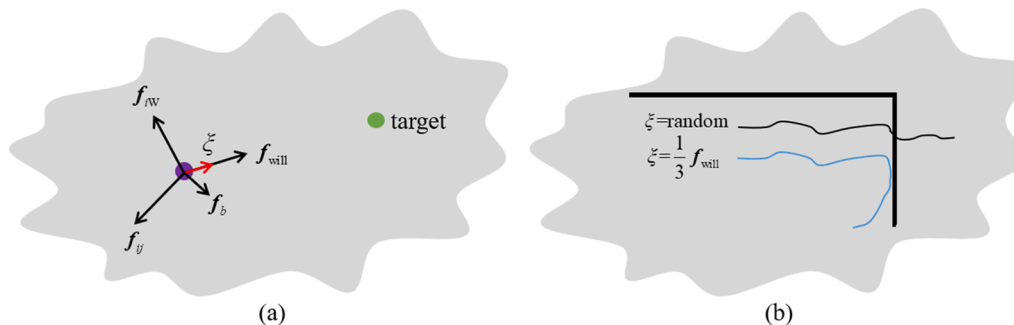


Fig. 4. Redefined random force.

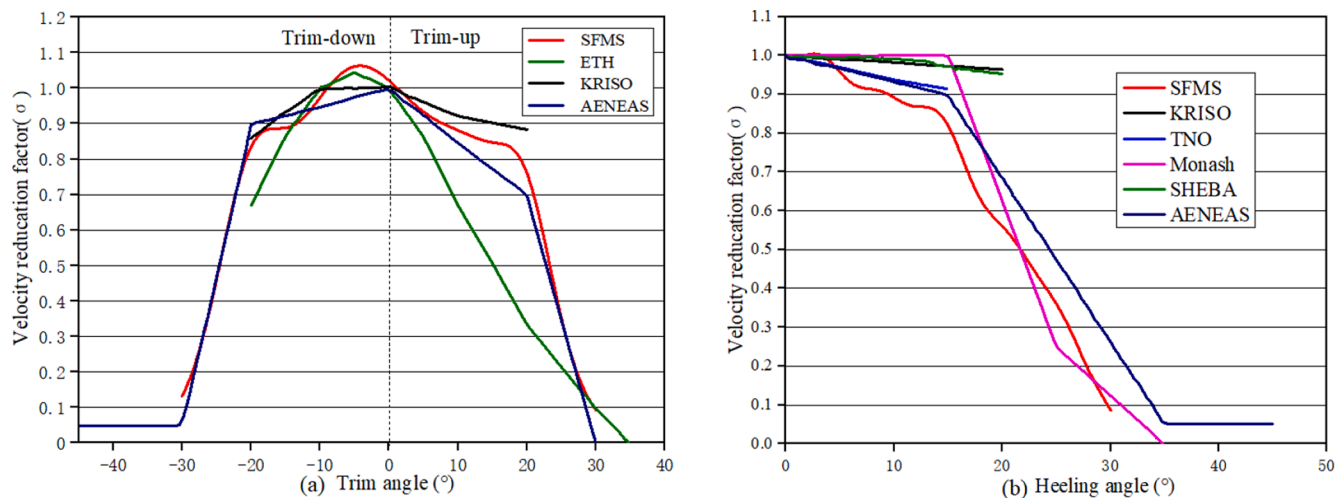


Fig. 5. Speed reduction factor under different trim and heeling angles.

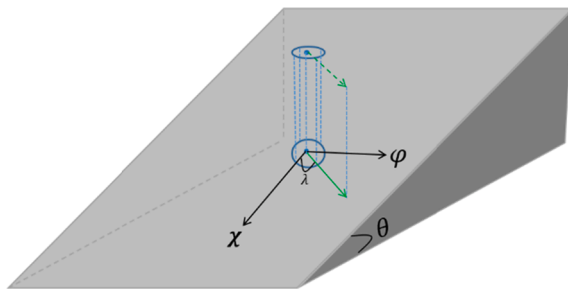


Fig. 6. Pedestrian moving direction on an inclined platform.

for any misleading results from this work.

Although there are some experimental records on the evacuation of inclined vessels, the inclination angles in practice can often reach approximately  $30^\circ$  in an emergency situation, which none of the previous experiments could not reach due to the safety reason. To address it, simulation has become one of the most effective research methods (Lovreglio and Kinateder, 2020; Song and Lovreglio, 2021). Kang et al. (2019) improved the SFM according to pedestrian dynamics and simulated different evacuation scenarios during a shipwreck. They explored the influence of the inclination angle and walking speed on the evacuation efficiency by simulation and found that the evacuation of pedestrians was the fastest when they walked along the inclined direction of a ship. In addition, some competitive pedestrians may accelerate the evacuation process and reduce the escape time. However, the process has a negative impact if there are too many competitive pedestrians. Based on the intelligent model for extrication simulation (IMEX), Kim et al. (2004) considered ship motion and inclination, increased the amount of psychological and physical forces on agents, and simulated the evacuation results of various scenarios during an emergency evacuation. Hamburgische Schiffbau-Versuchsanstalt (HSVA), based on the experimental research results of other organizations, including Korea Research Institute of Ship and Ocean Engineering (KRISO) (Lee et al., 2004), the Monash University in Australia (Brumley and Koss, 1998), the Netherlands Organization for Applied Scientific Research (TNO) (Bles et al., 2001), BMT Fleet Technology using the SHEBA simulator (Glen, 2004), and the Swiss Federal Institute of Technology (ETH) in Zürich (Weidmann, 1993), used the software named “AENEAS” to simulate ship evacuation at different inclination angles and submitted a report about the evacuation of inclined vessels to the IMO (Valanto, 2006). The report also proposed a reduction law of the walking speed with a slope angle, hereinafter referred to as the “HSVA report”. These

simulations usually only defined a single angle between the pedestrian movement direction and the inclined direction in a complete evacuation process. In fact, the influences of heeling and trim on an individual's speed are different, and the movement directions of passengers are constantly changing when evacuating in an inclined ship. As a result, the attenuation of speed by a combined effect of heeling and trim is also different. To address such shortcomings, speed attenuation is calculated synchronously at each time step, to eliminate errors caused by this problem in simulation.

To date, researchers have used ship corridor simulators or experiments for ship trial observations to study the impact of ship lists on individuals' walking speeds. There have however been limited studies on the impact of a ship listing angle on the evacuation time from a restricted area on ships, the state-of-the-art studies in the field are based on a hypothesis either that the evacuation environment is not an inclined vessel, or that they focus on the inclined corridors or stairs. Meanwhile, given the various improvements of SFM that have been widely used in the field of land-based evacuation, it is beneficial to incorporate ship inclinations into evacuation models. In view of this, an improved SFM is established to simulate the evacuation process from a public area/room of a passenger vessel under an inclined condition. This can fill the aforementioned research gap, and also ensure the safety of experiments under ship extreme conditions in an emergency. The contributions of this study lie in that:

- (1) The improved SFM aids to analyse the influence of different inclination angles on an individual's walking speed and the total evacuation time of all the involved personnel, under the circumstance that the angle between the direction of pedestrian movement and the direction of ship incline is constantly changing. This has the advantage of being able to describe more objectively the inclined influence on pedestrians in restricted areas (rooms) at each time step according to their moving direction.
- (2) The number of pedestrians in room may change due to some events, so the impact passenger density on walking speeds of pedestrians and total evacuation time are analysed. The scenarios are formulated through the study case of a canteen on a training ship, which studied the effects of a combination of inclination and density on evacuation results by changing the number of evacuees in the canteen.
- (3) The analysis of studies is conducted in special scenario with the “Guidelines” of IMO, the results emerged provide insights into the selection of proper evacuation timing and organization. Considering the compatibility of model, the improved SFM can be well

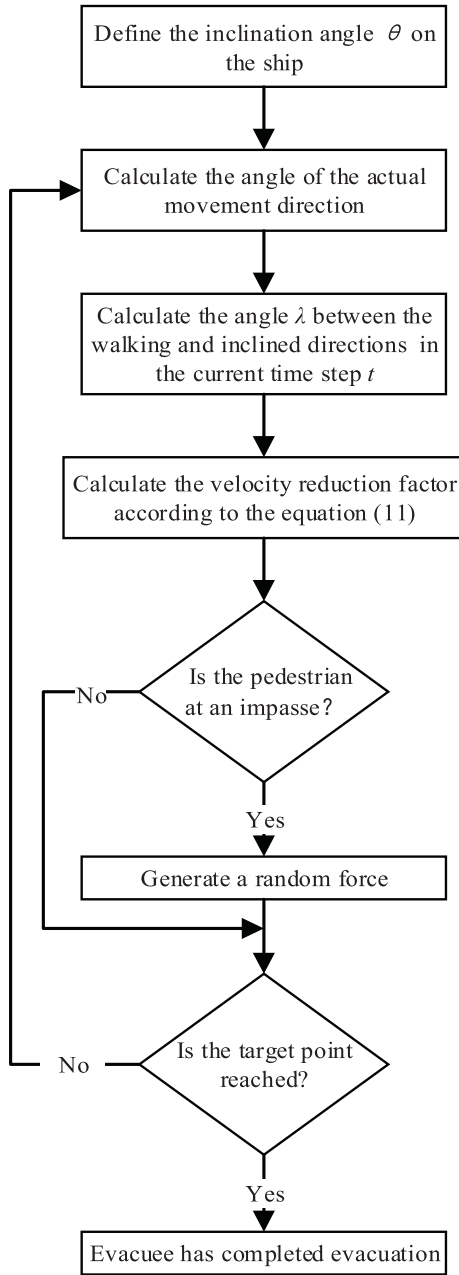


Fig. 7. The flowchart of the SFMS calculation.

coordinated with some evacuation software developed based on SFM, and the results also can be used as input parameters in software to be applicable to more complex and special scenarios.

### 3. Model and methods

#### 3.1. An improved SFM for ship inclination

The basic model used in this research is the SFM proposed by Helbing and Molnar (1995). The SFM is mainly composed of the desired force  $f_{will}$ , interaction force  $f_{ij}$ , wall force  $f_{iw}$  and random force  $\xi$ , as shown in Fig. 2. Under the action of the resultant force, it is assumed that the speed of pedestrian  $i$  is  $v_i(t)$  at time  $t$ ; then, a pedestrian with mass  $m_i$  will achieve an acceleration  $\frac{dv_i}{dt}$ , and the corresponding movement will satisfy Eq. (1).

$$m_i \frac{dv_i}{dt} = f_{will} + \sum_{j(j \neq i)} f_{ij} + \sum_w f_{iw} + \xi \quad (1)$$

In the model, the desired force  $f_{will}$  reflects that pedestrians are affected by targets or exits, and Eq. (2) expresses the desired force generated by a pedestrian in the process of moving towards a target point in the direction  $e_i^0$ . The pedestrian needs to adjust his/her current speed  $v_i(t)$  to the desired speed  $v_i^0(t)$  in the reaction time  $\tau_i$ .

$$f_{will} = m_i \frac{v_i^0(t)e_i^0 - v_i(t)}{\tau_i} \quad (2)$$

The interaction force mainly reflects the repulsion force generated by others, including the psychological repulsion force  $f_{ij}^{psychology}$ , extrusion force  $f_{ij}^{body}$  and friction force  $f_{ij}^{slide}$ , as shown in Eq. (3). If there is no contact ( $r_{ij} \leq d_{ij}$ , where  $r_{ij}$  is the sum of the radii of  $i$  and  $j$ ,  $d_{ij}$  is the distance between the pedestrians  $i$  and  $j$ ), only psychological repulsion force  $f_{ij}^{psychology}$  is generated to maintain a certain distance. In Eq. (4),  $A_{ij}$  and  $B_{ij}$  are the distance parameters. When the distance between  $i$  and  $j$  satisfies  $r_{ij} > d_{ij}$ , an extrusion force  $f_{ij}^{body}$  and a friction force  $f_{ij}^{slide}$  are generated through physical contact. The other parameters are explained as follows:  $k$  is the extrusion coefficient.  $n_{ij}$  is the unit vector of pedestrian  $j$  pointing towards pedestrian  $i$ .  $g(x)$  is a piecewise function in Eq. (5), where if there is physical contact between pedestrians ( $r_{ij} > d_{ij}$ ), then  $g(x) = x$ ; otherwise,  $g(x) = 0$ .  $\kappa$  is the friction coefficient.  $\Delta v_{jt_{ij}} (\Delta v_{jt_{ij}} = (v_j - v_i) \cdot t_{ij})$  is the speed difference between two pedestrians in the tangential direction, where  $t_{ij}$  ( $t_{ij} = (-n_{ij}^2, n_{ij}^1)$ ) indicates the unit vector in the tangential direction.

$$f_{ij} = f_{ij}^{psychology} + f_{ij}^{body} + f_{ij}^{slide} \quad (3)$$

$$f_{ij} = [A_{ij} \exp(\frac{r_{ij} - d_{ij}}{B_{ij}}) + k g(r_{ij} - d_{ij})] n_{ij} + \kappa g(r_{ij} - d_{ij}) \Delta v_{jt_{ij}} \quad (4)$$

$$g(x) = \begin{cases} x & r_{ij} > d_{ij} \\ 0 & r_{ij} \leq d_{ij} \end{cases} \quad (5)$$

Similarly,  $f_{iw}$  is the force of the boundaries (such as wall  $w$ ) on pedestrian  $i$ . In Eq. (6),  $d_{iw}$  means the distance from the pedestrian  $i$  to the wall  $w$ ,  $n_{iw}$  denotes the perpendicular direction to the wall, and  $t_{iw}$  is the tangential direction, also,  $A_{iw}$  and  $B_{iw}$  are the distance parameters. This force is similar to the force  $f_{ij}$  between pedestrians, including the psychological repulsion force  $A_{iw} \exp(\frac{r_i - d_{iw}}{B_{iw}}) n_{iw}$ , extrusion force  $k g(r_i - d_{iw}) n_{iw}$  and friction force  $\kappa g(r_i - d_{iw}) (v_i \cdot t_{iw}) t_{iw}$ , wall force is not redefined here (Helbing and Molnar, 1995; Kang et al., 2019; Ma et al., 2019).

$$f_{iw} = [A_{iw} \exp(\frac{r_i - d_{iw}}{B_{iw}}) + k g(r_i - d_{iw})] n_{iw} + \kappa g(r_i - d_{iw}) (v_i \cdot t_{iw}) t_{iw} \quad (6)$$

Compared with flat terrains, when a ship is inclined, pedestrians need to overcome the influence of the incline while walking along a slope (Lovreglio et al., 2019). As shown in Fig. 3, the inclination angle is  $\theta$ , and a pedestrian receives an inclined force  $f_b$  along the inclination direction when walking along the  $\lambda_1$  and  $\lambda_2$  directions, which is caused by the component force  $f_b$  of his/her own gravity  $G$ , where  $f_b = G \times \sin\theta = m_i g \sin\theta$ ,  $g$  is gravitational acceleration. As an extra force in the inclined space,  $f_b$  is in the same dimension as the other forces, and can be used for vector calculation with others. It ensures that it can be incorporated into basic SFM.

In real life, if only the inclination force is added to the SFM, the moving speed of pedestrians may continue to accelerate or decelerate, which is obviously inconsistent with the objective reality. However, the impact varies according to the inclination degree in reality. Pedestrians can overcome the adverse effects of an inclined state with different body adjustment forces; thus, the self-adjustment force  $f_{adj}$  of pedestrians under different inclined situations should be added. The SFM of a ship

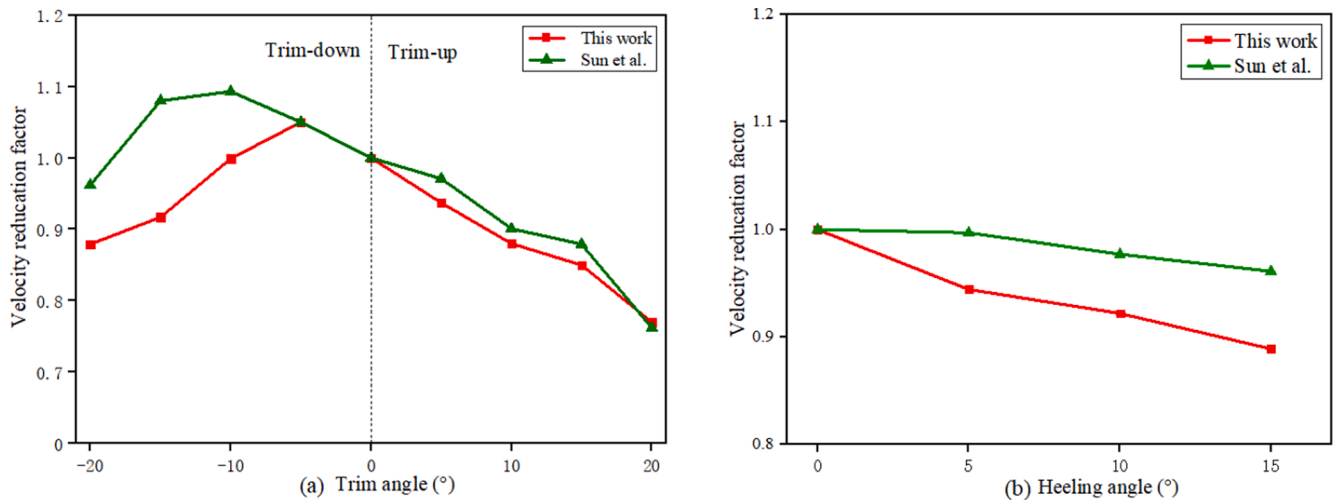


Fig. 8. Comparison of the speed reduction factors in this study and those in trim and heeling experiments.

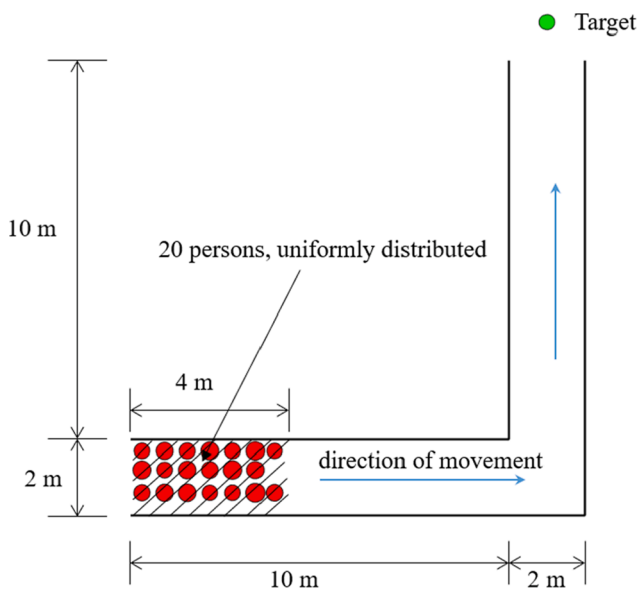


Fig. 9. Configuration rounding corner of test 6 in the “Guidelines”.

(SFMS) is thus established, as shown in Eq. (7).

$$m_i \frac{dv_i}{dt} = f_{will} + \sum_{j(j \neq i)} f_{ij} + \sum_W f_{iW} + f_b + f_{adj} \quad (7)$$

When a pedestrian walks in the direction  $\lambda_1$  in Fig. 3, it is similar to walking on a downhill slope. Due to the effect of the inclination force (gravity component), the pedestrian always accelerates along the slope if considering only the inclination force. In real life, pedestrians may change their centre of gravity backward by their self-adjusting force  $f_{adj}$  to avoid rolling and other dangerous behaviours caused by excessive forward lean. Similarly, in the process of walking along an uphill slope, they may stop moving when the inclination angle reaches approximately  $15^\circ$  without considering the self-adjustment force calculated using Eq. (8). However, it is found that they can overcome the  $15^\circ$  slope in reality. Therefore,  $f_{adj}$  is the force needed to adjust their own pace with the help of handrails and other auxiliary equipment at this time. When a pedestrian walks in the direction  $\lambda_2$ , as shown in Fig. 3, the inclined effect of heeling affects the pedestrian walking in the left or right direction. At this time, his/her walking trajectory is a curve that is biased to the inclination direction if the self-adjusting force is not added. At this

exact moment, the pedestrian needs to use  $f_{adj}$  to correct his/her body state, especially when the inclination angle is too large, and must choose to hold onto a handrail to avoid his/her body leaning too much to one side, which usually leads to a decrease in walking speed. In the model, in order to better represent the movement of personal on an inclined ship by the equations, the angle  $\lambda$  between the inclined direction of the ship and the walking direction of personal is used to represent the traditional heeling and trim. For example, when the ship has a traditional trim, walking along the short axis or athwartship axis of the ship ( $\lambda = 90^\circ$ ) is called heeling, and walking along the long axis or fore-aft axis of the ship ( $\lambda = 0^\circ$  or  $180^\circ$ ) is called trim. When the ship has a traditional heeling, walking along the short axis or athwartship axis of the ship ( $\lambda = 0^\circ$  or  $180^\circ$ ) is called trim, and walking along the long axis or fore-aft axis of the ship ( $\lambda = 90^\circ$ ) is called heeling. Here, a positive trim angle represents pedestrians uphill walking, while a negative one means downhill. In addition, considering the small difference between heeling to the left or right of pedestrians, the positive and negative of heeling angles are not distinguished.

$$f_{will} + \sum_{j(j \neq i)} f_{ij} + \sum_W f_{iW} = f_b = G \times \sin\theta \quad (\theta \approx 15^\circ) \quad (8)$$

### 3.2. Selection of the random force

In the existing SFM or improved SFM research, previous studies (Sticco et al., 2020; Sticco et al., 2021) found that the parameters of the model also have a direct effect on the result accuracy. As a constant in the model, random force is often neglected in a simulation process. More specifically, there are rare studies in the literature that focus on choosing the appropriate model of random force with respect to a specific scenario. However, it is found that pedestrians sometimes try to pass through walls or obstacles and other unreal phenomena in simulations. Additionally, a pedestrian may reach an equilibrium state if the received resultant force is 0, and then the stop behaviour may occur. In real life, evacuees tend to solve the dilemma by increasing the desired force or psychological force exerted by walls or obstacles. In view of this phenomenon, appropriate random forces are selected as alternative methods to address these special behaviours in SFMS. As shown in Fig. 4 (a), the resultant force of all the forces (that is, the forces represented by the black arrows) on the pedestrian in the SFMS is 0. At this point, if there is no additional random force, the pedestrian may stop moving or make reciprocating movements within a certain range. In the SFMS, an additional random force (the force represented by the red arrow in Fig. 4 (a)) needs to be generated in the model simulation. Once the equilibrium state is broken, the random force is immediately discarded. To ensure

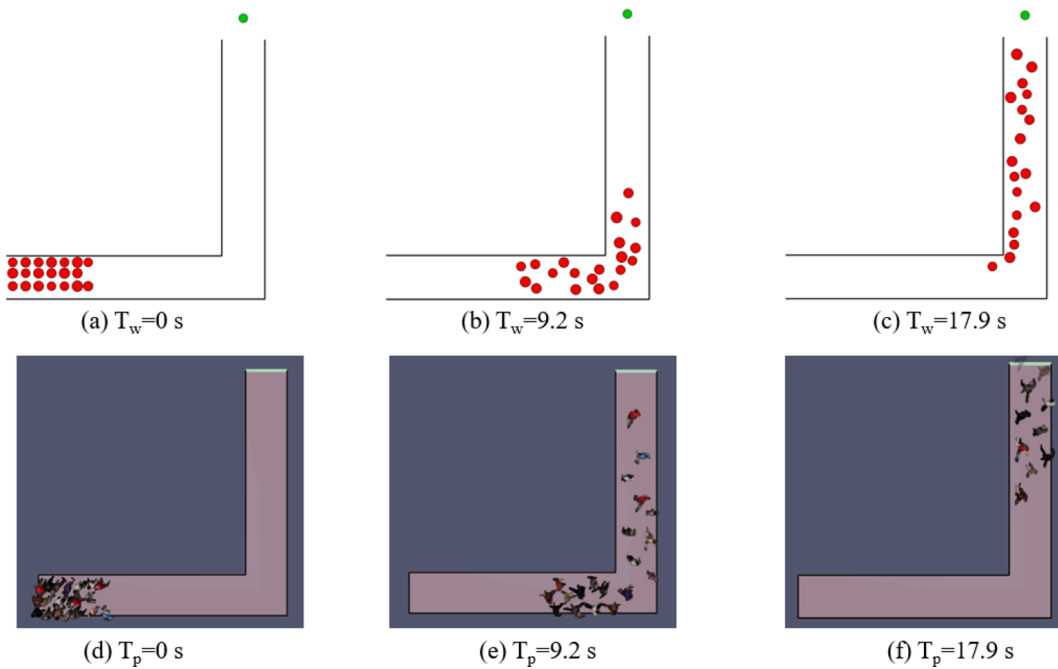


Fig. 10. Comparison of the results in this study and obtained using Pathfinder.

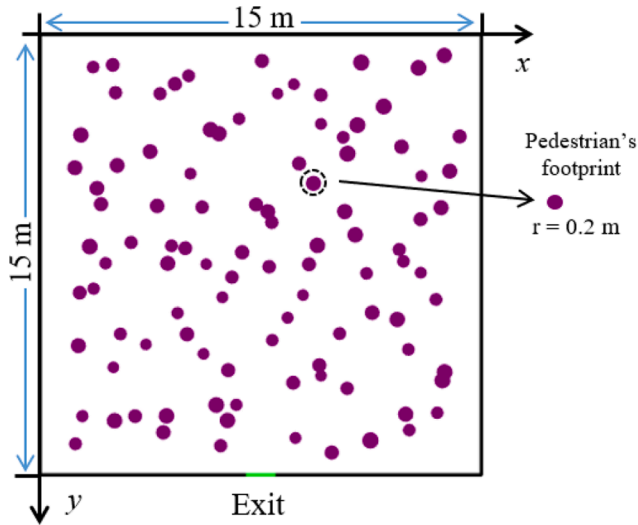


Fig. 11. Distribution of pedestrians in a room when N = 100.

the reliability of the simulation, the random force is set to 0 under normal circumstances. When the resultant force on the pedestrian is 0 in three consecutive time steps, the pedestrian is considered to be in deadlock, and the random force  $\xi$  is generated. In this case, the location of the pedestrian is always closer to the wall, as shown in Fig. 4(b), the pedestrian may try to cross the wall if the direction of the random force is chosen randomly. It is crucial to choose the suitable direction of random force to ensure that the pedestrians near a boundary are still in the evacuation area at the next time step (Anvari et al., 2015; Dias et al., 2018). Therefore, choosing the direction of random force to be consistent with the direction of desired force  $f_{will}$  can effectively address this issue. As for the magnitude of random force, it is found that system run most smoothly when  $\xi = \frac{1}{3}f_{will}$  by tests, and the magnitude of random force has little influence on the overall evacuation results because the time step in the model is small enough to be  $10^{-6}$  s. More details on random force tests can be found in Table 1 of Appendix A. Furthermore,

this pedestrian with concern may stop moving and random force is not generated until there is enough space around for him/her to occupy (Fang et al., 2021).

### 3.3. Speed reduction factor

The speed of pedestrians often decreases to a certain extent under the influence of ship inclination. However, considering the safety and effectiveness of experiments, the speed attenuation cannot be measured when the actual slope angle is large. Also, there is currently no unified definition of the speed reduction under an inclined condition. Therefore, the inclination angle continuously increases from  $0^\circ$  to  $30^\circ$  at a step of one degree in SFMS, and the average reduction factor of an individual's walking speed is recorded, see Table 2 in Appendix B for more details. Eq. (9) and Eq. (10) are the best expressions of trim and heeling for accurately describing the reduction factor of speed at a particular angle by data fitting respectively. In Eqs. (9) and (10),  $\sigma(\theta)$  and  $\sigma(\theta_\perp)$  are the speed reduction factors on the trim and heeling, respectively while  $e$ , and  $f$ , and  $g$  correspond to the fitting constants. More details on fitting data and constants can be seen in Appendix B.

$$\sigma(\theta) = \sum_{i=1}^4 e_{\theta_i} \exp\left(-\left(\frac{\theta - f_{\theta_i}}{g_{\theta_i}}\right)^2\right) \quad (9)$$

$$\sigma(\theta_\perp) = \sum_{i=1}^4 e_{\theta_\perp i} \exp\left(-\left(\frac{\theta_\perp - f_{\theta_\perp i}}{g_{\theta_\perp i}}\right)^2\right) \quad (10)$$

Fig. 5 shows a comparison of the speed attenuation curve with the inclination angle between the SFMS and "HSVAreport" which refers to the experimental results of other institutions and the speed attenuation simulated by the evacuation software AENEAS (Bles et al., 2001; Brumley and Koss, 1998; Glen, 2004; Lee et al., 2004; Valanto, 2006; Weidmann, 1993). Through the comparison of those results, it is found that the speed reduction factors produced by SFMS are highly consistent with the variation trend of the simulations and real experiments. It can prove that the SFMS is reliable for pedestrian speed attenuation under different inclination conditions.

As shown in Fig. 5(a), in the case of a small trim angle, when walking along a downhill slope, the walking speed of a pedestrian will accelerate

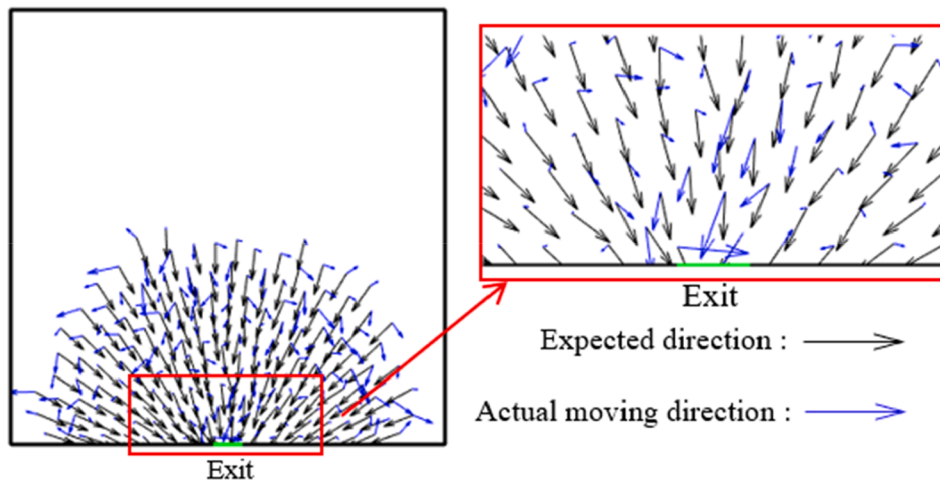


Fig. 12. Moving vectors when  $T = 5$  s.

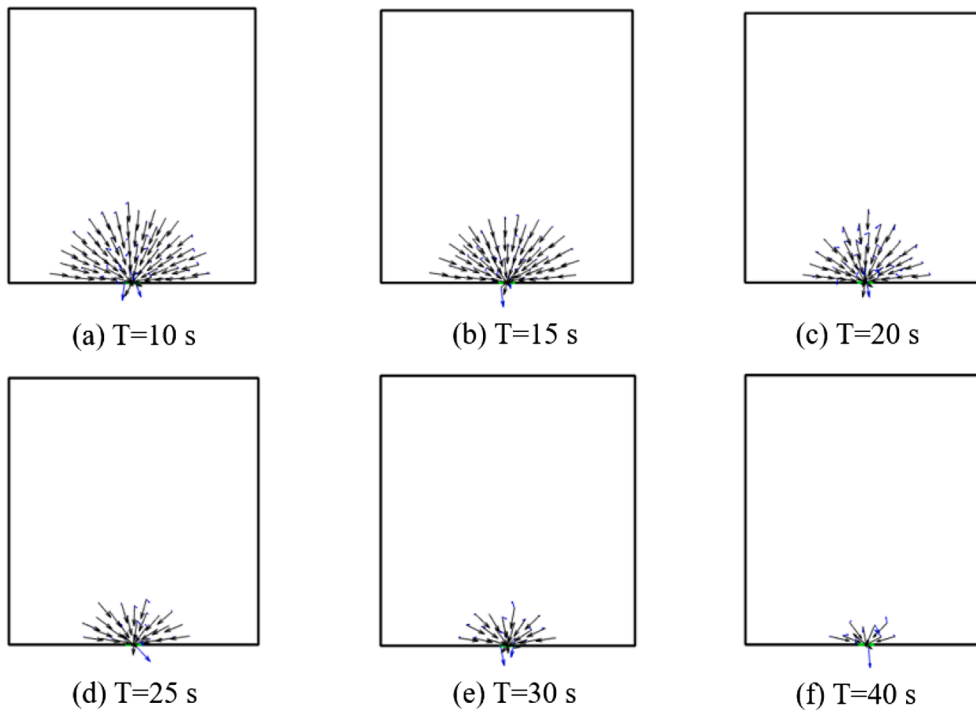


Fig. 13. Moving vector of overall evacuation process.

to a certain extent. Considering a real-life situation, the maximum angle is set to  $30^\circ$ . From Fig. 5(a) and 5(b), it can be found that, at the same angle, the heeling has a greater impact on the speed compared with the trim, especially when the inclination angle exceeds  $15^\circ$ , at which point the speed begins to drop steeply.

In the evacuation process, the expected directions of pedestrians are in general from a dangerous area towards evacuation exits, but the actual moving directions are not always consistent with the expected ones because of waiting congestion, squeezing and other behaviours (Bartolucci et al., 2021). However, the speeds of pedestrians in different moving directions are affected by the inclination differently when walking on a slope. Therefore, the angle between the direction of movement and the direction of inclination is defined in the SFMS model (Kang et al., 2019). As shown in Fig. 6, the slope angle is  $\theta$ , the inclination direction along the slope is indicated by the arrow  $\chi$ , and the green dotted arrow is the pedestrian walking direction. Since the direction of pedestrian movement and the inclination direction constitute

an angle in a three-dimensional space, for the convenience of calculation, the direction of pedestrian movement is projected onto the inclined plane, as a solid arrow shown in Fig. 6.  $\lambda$  is the angle between the pedestrian walking direction and the direction of inclination. When the pedestrian walking direction is the same as the inclination one, that is,  $\lambda = 0^\circ$ , pedestrians are affected only by the trim in this scenario, and the reduction in the speed factor is  $\sigma(\theta)$ . Similarly, when  $\lambda = 90^\circ$ , the pedestrian walking direction is perpendicular to the inclination one, as shown by the arrow  $\varphi$  in Fig. 6. At this time, the speed is mainly affected by the heeling, and the reduction factor is  $\sigma(\theta_\perp)$ . However, pedestrians may be affected by both heeling and trim under real circumstances. As a result, in this case, the spatial interpolation method is used to calculate the speed reduction factor in the SFMS, as shown in Eq. (11). The main reason of using this method is that it makes it possible to obtain the speed attenuation factor for the non-specific moving direction as accurately as possible, while keeping the calculation simple. For example, when  $\lambda$  is  $\frac{\pi}{4}$ , heeling  $\sigma(\theta_\perp)$  and trim  $\sigma(\theta)$  have the same effect on speed,

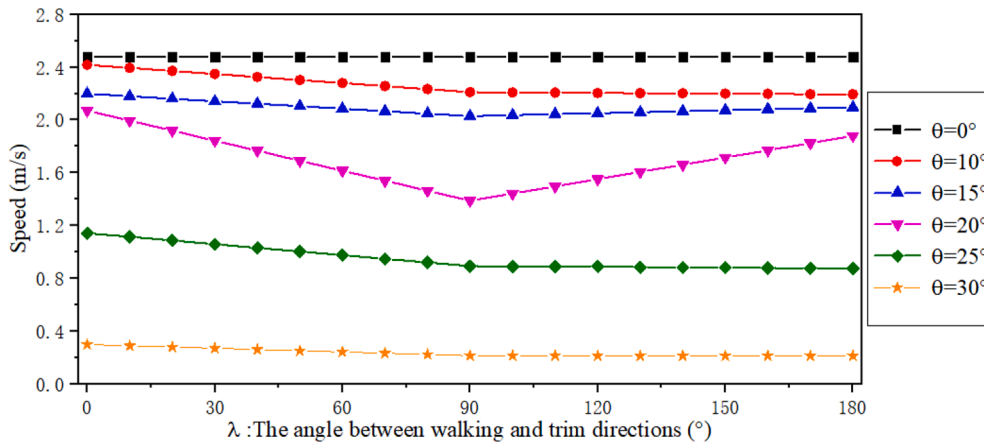


Fig. 14. The walking speed of passenger under different λ at various trim angles.

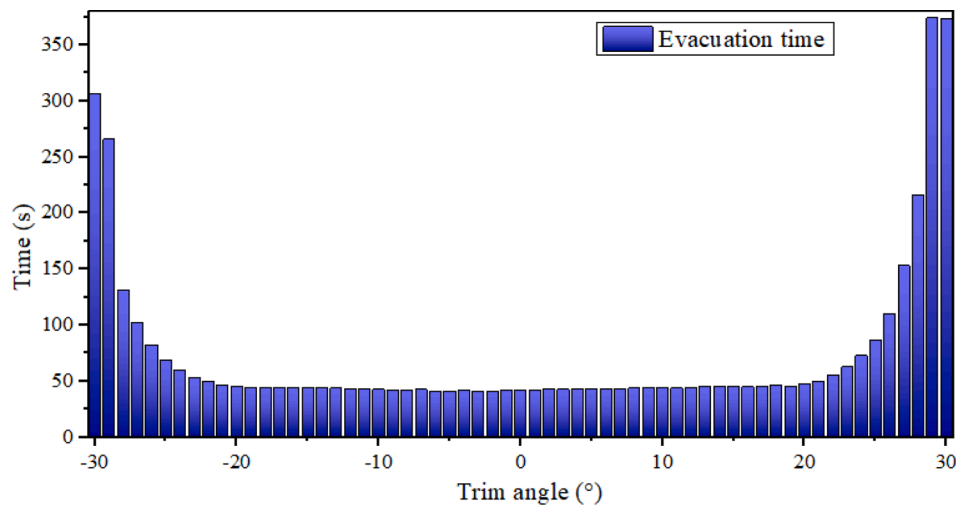


Fig. 15. Average evacuation time of 100 evacuations at different inclination angles.

and the reduction factor is  $\sigma = \frac{1}{2}\sigma(\theta_{\perp}) + \frac{1}{2}\sigma(\theta)$ .

$$\sigma = \frac{2\lambda}{\pi}\sigma(\theta_{\perp}) + \frac{\pi - 2\lambda}{\pi}\sigma(\theta) \quad (11)$$

In the process of the SFMS simulation, under a certain ship inclination angle, agents make a judgement on the angle λ according to their own moving direction in each time step, determine the attenuation of the speed, and obtain their individual walking speeds of the current time step. In addition, the issue as to whether a person is stuck in a stalemate needs to be determined to generate the corresponding random force. If the generated random force cannot solve the impasse, a new resultant force will be calculated as the position of surrounding pedestrians moves. At this time, it is necessary to judge whether the pedestrian is still stuck in a stalemate, to determine whether the random force will be generated until the exit is reached. The specific SFMS operation process is shown in Fig. 7.

The above improvement can also be applied to the simulation software developed by SFM. First, the simulation scenario should be established according to the ship layout, and users can input the trim or heeling angle and other parameters. The moving directions of pedestrians are determined synchronously at each time step. Then the attenuation factor of speed can be calculated by updating the force function, and a new walking speed is assigned to the agent in the inclined environment. Finally, the evacuation results are obtained.

#### 4. Verification

To verify the passenger behaviour model proposed in this study, two verification methods are adopted, namely, comparing with experimental reports in relevant literature and with the results from other established evacuation software respectively. As for the key parameters, detailed individual characteristics of each pedestrian can be given, for example, the optimal desired speed in emergency is set as  $v_i^0 = 2.48$  m/s (Ma et al., 2019). According to current human dimensions of Chinese adults (CNIS, 1988), the pedestrian parameters are set as: mass  $m = 80$  kg and radius  $r = 0.2$  m (both  $m$  and  $r$  satisfy a normal distribution). By referencing previous studies (Helbing et al., 2000; Helbing and Molnar, 1995), the rest of the variable values of the SFMS are set as follows:  $k = 1.2 \times 10^5$ ,  $\kappa = 2.4 \times 10^5$ ,  $A = 2.0 \times 10^3$ ,  $B = 0.08$ , and  $\tau_i = 0.5$  s. All the simulations were run on a laptop with an Intel (R) Core (TM) i7 3.7 GHz CPU, Nvidia GTX 1080 GPU, and 64 GB of memory.

##### 4.1. Experimental verification reported in relevant literature

Experimental results obtained by Sun et al (2018a) were used as references to verify the reliability of SFMS in heeling and trim environments. They used a ship corridor simulator with the size of 10.0 m (L) × 1.8 m (W) × 2.2 m (H) to study the effects of heeling and trim on walking speeds. Similarly, SFMS is used to establish the same experimental environment, and the comparisons of results are shown in Fig. 8. The green line represents Sun et al (2018a)'s experimental results, which

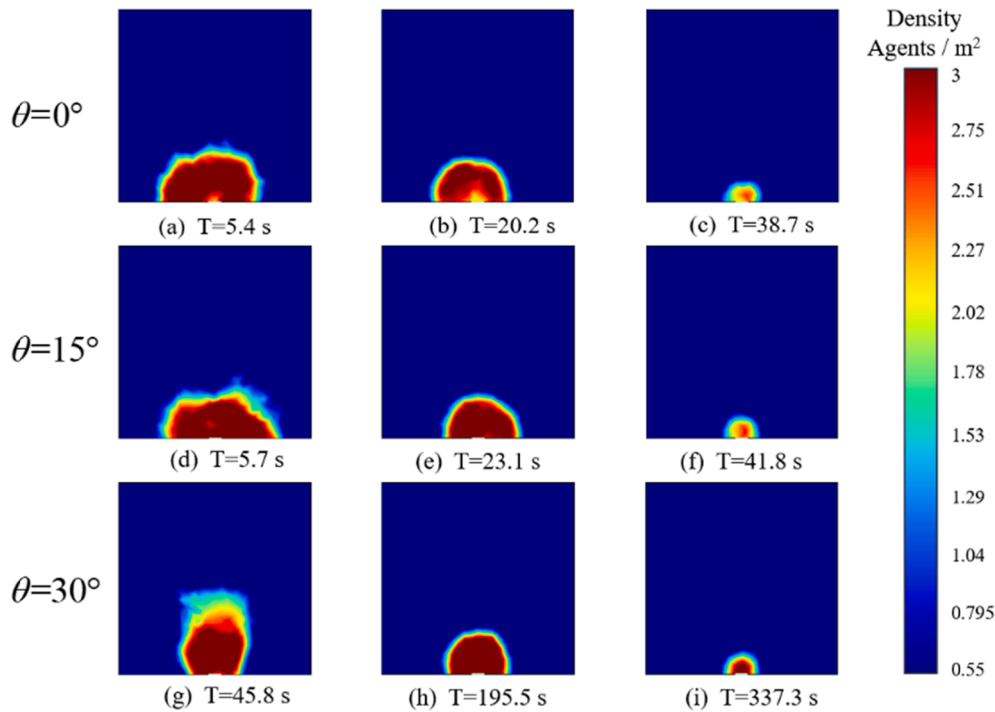


Fig. 16. Density distribution heatmap of evacuees at different stages in the room at various trim angles.

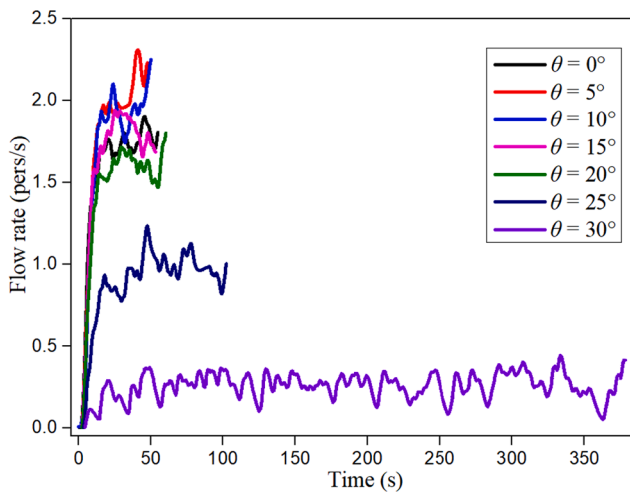


Fig. 17. Flow rate at exit.

were obtained by averaging the speeds of 17 participants in each scenario. Furthermore, the speed attenuation factor in simulation is consistent with the variation trend of Sun et al (2018a)'s experiment in both heeling and trim scenarios. It can be verified that parameter settings are valid. The small variation in terms of the data probably results from the participants' difference between the two experiments. The participants in Sun et al (2018a)'s experiment were mostly young students, and they should be relatively less affected by heeling and trim than the general population.

#### 4.2. Verification of the rounding corners of test 6 in the IMO Guidelines

To further strengthen the validation of SFMS, a typical test recommended by the "Guidelines" is used to validate the feasibility of the model (Ha et al., 2012). In similar studies (Ni et al., 2017; Park et al., 2015), the "Guidelines" test 6 was used to verify the applicability of the

model, since it can be observed whether pedestrians cross boundaries and overlap when walking in a group of people and whether pedestrians can walk smoothly at the corner. The configuration of test 6 in association with the "Guidelines" is shown in Fig. 9, and the test investigate how twenty persons approaching a left-hand corner will successfully navigate around the corner without penetrating the boundaries. The shaded area in Fig. 9 is the starting area, and the blue arrow represents the direction of movement. However, the "Guidelines" did not provide a reference standard for evacuation time, and the evacuation software Pathfinder is used to build an identical scenario to verify the reliability of our work.

The evacuation processes of two models are shown in Fig. 10, where (a), (b), (c) represent the snapshots of SFMS and (d), (e), (f) are snapshots of evacuation software Pathfinder. At the beginning of the evacuation, 20 pedestrians were uniformly assigned to the starting area. It is confirmed that pedestrians in SFMS can successfully reach the target without colliding with others and penetrating boundaries. Also, there are similar distributions of pedestrians in the processes compared to the results of Pathfinder. Pedestrians in SFMS have some time lag in their evacuation, and it may be caused by setting of the different parameters. Here, each "time" thereafter refers to the simulation clock time.

## 5. Case study

The training vessel "YUKUN" of Dalian Maritime University which can accommodate 240 students, is taken as the research object in this study. The public area/room (restaurant) size on MV "YUKUN" is 15 m  $\times$  15 m, and for activities such as dancing parties, it can accommodate >250 students and crew. The width of the exit of the restaurant is approximate 1 m. Also, this experiment well fits the simulation scheme in the defined test 9 of the "Guidelines", in which the size of the model room without obstacles is recommended as length of 30 m, width of 20 m, and exit width of 1 m. Test 9 mainly aims to explore the rule of crowd dissipation from a public room, and the influence of tables or chairs in the room on results is not taken into account. The same setting is also applied to this case. To ensure that the whole evacuation process best reflects the reality, the size of the simulation room is set as 15 m  $\times$  15 m,

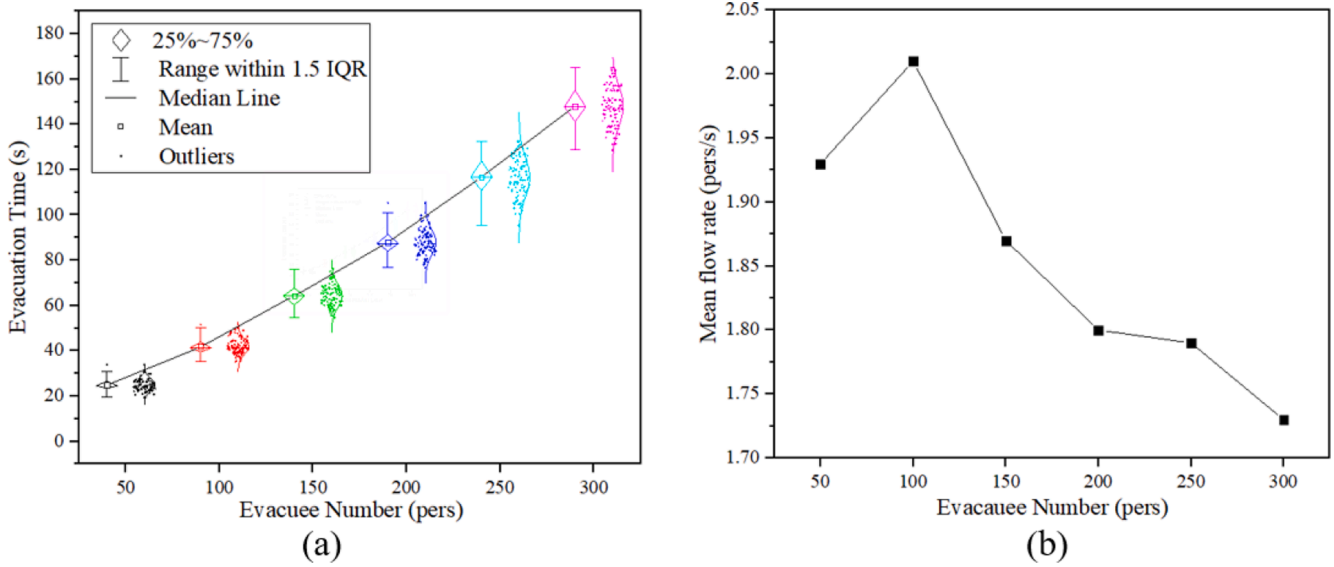


Fig. 18. Evacuation time and mean flow rate of various numbers of passengers without inclination.

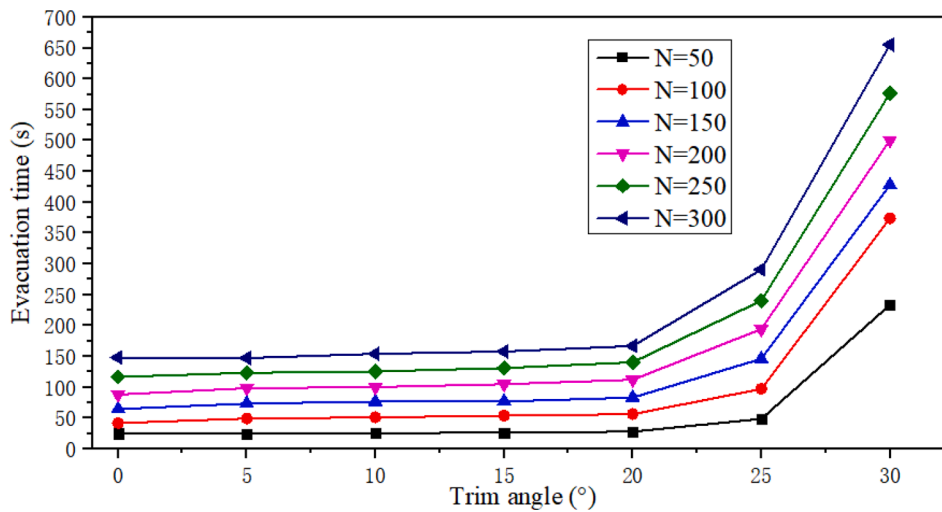


Fig. 19. Evacuation time of different numbers of people in various trim angles.

Table 1

Tests for random force  $\xi$ .

$\xi$	Run times	Times of penetrating boundaries	Times of still at an impasse	Mean displacement
random	100	32	27	0.34
$f_{will}$	100	17	3	1.05
$1/2 f_{will}$	100	6	4	0.67
$1/3 f_{will}$	100	0	0	0.11
$1/4 f_{will}$	100	0	7	0.09
$1/3 f_{wall}$	100	12	31	1.23
$1/3 f_j$	100	69	0	0.48

and the number of pedestrians (N) in the room is set differently. The response duration distribution for passengers is assumed to be the day cases provided by the “Guidelines”. Since the initial positions and some parameters are generated randomly, the simulations of each scenario are simulated 100 times by MATLAB to eliminate random errors and outliers. The most appropriate and representative result is selected by averaging all simulation results.

Fig. 11 illustrates a random distribution of evacuees in a room when N = 100, where the size of each circle is determined by the radius of the

pedestrian’s footprint. The y direction points towards the bow, and x refers to the port side, indicating the athwartship direction. The exit is shown as a green line, the width (D) of which is set as 1 m. Fig. 12 is a vector graph of pedestrian movement in the room when the evacuation time T = 5 s, where the black arrow represents the expected direction of each pedestrian, the blue arrow represents the current actual moving direction and speed, and the starting point of each arrow is the current position of each pedestrian. Other vector graphs of evacuation process are shown in Fig. 13, which prove that agents successfully gather towards the exit without overlapping or penetrating the boundaries.

### 5.1. Evacuation results on an inclined ship

Fig. 14 shows the influence of different walking directions and vessel inclination angles (heeling and trim) on resultant walking speed, it is assumed that inclination refers to ship’s trim. The angle  $\lambda$  is taken as the independent variable and varies as  $\Delta\lambda = 10^\circ$ . In general, the walking speed decreases with increasing inclination, and there is no change in speed in each moving direction without inclination, which is 2.48 m/s. When  $\theta = 10^\circ$ , the speed slightly decreases with increasing  $\lambda$  because pedestrians walk downhill similarly, and they can effectively control

**Table 2**  
The speed reduction factor at different heeling and trim angles in SFMS.

Heeling angle	Speed reduction factor	Trim angle	Speed reduction factor	Trim angle	Speed reduction factor
0°	1	-30°	0.12208	1°	0.98558
1°	0.99792	-29°	0.17494	2°	0.97313
2°	1.00039	-28°	0.23641	3°	0.95976
3°	1.00009	-27°	0.30684	4°	0.9511
4°	1.00102	-26°	0.38398	5°	0.93785
5°	0.9443	-25°	0.46059	6°	0.92587
6°	0.93113	-24°	0.54054	7°	0.91106
7°	0.9224	-23°	0.62604	8°	0.90076
8°	0.90951	-22°	0.70943	9°	0.88753
9°	0.90296	-21°	0.79054	10°	0.88085
10°	0.88966	-20°	0.86067	11°	0.87063
11°	0.8831	-19°	0.86407	12°	0.86405
12°	0.8706	-18°	0.8717	13°	0.85888
13°	0.85924	-17°	0.87926	14°	0.85275
14°	0.85152	-16°	0.88487	15°	0.84519
15°	0.84345	-15°	0.89182	16°	0.83758
16°	0.73591	-14°	0.89961	17°	0.83144
17°	0.68511	-13°	0.90583	18°	0.82492
18°	0.63702	-12°	0.91565	19°	0.8198
19°	0.59388	-11°	0.91867	20°	0.77112
20°	0.55149	-10°	0.99912	21°	0.68753
21°	0.52641	-9°	1.01276	22°	0.60259
22°	0.4915	-8°	1.02256	23°	0.52081
23°	0.44449	-7°	1.0333	24°	0.43793
24°	0.40156	-6°	1.04504	25°	0.36314
25°	0.35714	-5°	1.05005	26°	0.28613
26°	0.31286	-4°	1.05663	27°	0.21374
27°	0.24744	-3°	1.0632	28°	0.15605
28°	0.18834	-2°	1.07039	29°	0.11055
29°	0.13277	-1°	1.07507	30°	0.09621
30°	0.08771	0°	1		

their speed on this small slope. When  $\lambda$  is close to  $90^\circ$ , pedestrians are mainly affected by the horizontal inclined force, and the attenuation of their speed is relatively large. This effect is also reflected in  $\theta = 15^\circ$ , most likely because 1) the impact of the trim on pedestrians' moving speed is not different from that of heeling in the case of a small inclination angle and 2) the reduction in speed is not significant. As the trim angle increases to  $20^\circ$ , the impact of heeling on pedestrians is significant, and the minimum desired speed is 1.39 m/s at  $\lambda = 90^\circ$ , which is reduced by approximately 33% compared with 2.07 m/s at  $\lambda = 0^\circ$ . When the trim angle  $\theta$  is large than  $20^\circ$ , the speed of pedestrians is greatly affected by trim and decreases significantly. The difference between the speed attenuation caused by trim and heeling decreases again. As shown in Fig. 14, there are slight changes on the speed curves when  $\theta = 25^\circ$  and  $\theta = 30^\circ$ . The results are similar to the report by RIME (Yoshida et al., 2001) and NMRI (Murayama et al., 2000). By contrast, Sun et al. (2018a) reported that under normal walking and fast walking conditions, the effect of the trim on speed attenuation is often greater than that of heeling, which is not consistent with the conclusion of this study. The reason is probably due to the fact that the design and conditions of their experiments refer to inclined corridors. Also, the characteristics of evacuees (mass and psychology) and the frequency of tests are among the factors influencing different experimental results.

The trim angle ranges from  $-30^\circ$  to  $30^\circ$  to analyse the effect of the ship trim on the overall evacuation time. To better distinguish trim by head from stern, trim by head is defined as a positive value. Since the exit is located towards the bow, the evacuation time is different at the same trim angle under positive and negative trims. As shown in Fig. 15,  $N = 100$ ,  $D = 1$  m, and the variation curve of the speed with the trim angle is obtained according to the SFMS. For the overall evacuation process, a small speed attenuation has no significant effect on the evacuation time. When the trim angle is less than  $20^\circ$ , the evacuation time does not increase significantly in either the positive or the negative direction. However, when the angle exceeds  $20^\circ$ , the evacuation time

begins to change exponentially. When the trim angle is  $30^\circ$ , the evacuation time reaches the longest, i.e., 374 s. Compared with the curve of the speed reduction factor (Fig. 14), although the speed is only 56.0% of the desired speed at  $\theta = 20^\circ$ , the evacuation time does not increase significantly.

An observation of the whole evacuation process shows that the exit easily causes a large area of pedestrian congestion. As shown in Fig. 16 (a), when  $N = 100$ ,  $\theta = 0^\circ$ , and  $T = 5.5$  s, 10% of pedestrians complete the evacuation (initial stage), while the rest gather near the exit to wait for escape, forming serious congestion. This state continues until  $T = 20.2$  s, when half of the pedestrians have left the room (middle stage), as shown in Fig. 16(b), but there is still congestion at the exit. As shown in Fig. 16(c), when  $T = 38.7$  s, 90% of the pedestrians in the room complete the evacuation (end stage), and the congestion near the exit is alleviated.

Fig. 16(d), (e), (f) and (g), (h), (i) are the evacuation stages when  $\theta = 15^\circ$  and  $\theta = 30^\circ$ , respectively. Compared with the evacuation process without a trim angle, the increase in evacuation time is not significant at the initial stage (Fig. 16(d)), middle stage (Fig. 16(e)) and end stage (Fig. 16(f)) when the trim angle is  $15^\circ$ . Although congestion occurs at the exit, the duration is not different from that without trim, which indicates that  $\theta = 15^\circ$  has little effect on the overall evacuation process. However, when the trim angle reaches  $30^\circ$ , the duration of the evacuation time increases significantly, especially at the initial stage (Fig. 16(g)). It is found that the evacuation time increases to 45.8 s, and the density shows obvious stratification due to the slower speed. There is a group of pedestrians far from the exit who have not entered the congested area and do not wait in line. After 149.7 s, the evacuation reaches the middle stage at this trim angle, and the evacuees gather near the exit. The 50% pedestrian distribution area may be slightly smaller than that of other trim angles in the same stage. In general, severe trim, for instance  $\theta = 30^\circ$ , brings many adverse effects on the evacuation process, resulting in a longer duration of congestion and a sharp increase in the overall evacuation time.

To study the evolution of the evacuation process at different trim angles in detail, the change in the flow rate of pedestrians at the exit is recorded. Fig. 17 shows the variation of the exit flow rates with different trim angles and time when  $N = 100$ . It can be found that with increasing trim angles, the flow rate decreases correspondingly. When there is no inclination, the speed experiences no reduction, and the flow can reach 2–3 persons/s. When there is a small trim, the flow rate increases slightly from  $5^\circ$  to  $15^\circ$ . At this time, the exit reaches the optimal state due to the decrease in speed, which also verifies the phenomenon of "fast-is-slow" (Helbing et al., 2000). In addition, it is because that the flow rate continuously increases at the initial stage of almost all the cases (except for the case of  $\theta = 30^\circ$ ), and then reaches a saturation and begins to fluctuate. The reason is probably because that some passengers close to the door are not affected by the congestion and can evacuate more smoothly at the initial stage. As passengers gradually gather at the exit, evacuees escape from the room in disorderly fashion, which results in the fluctuation of the flow rates.

Intriguingly, similar to the results of individual speed, the flow rate at the exit also decreases significantly when the trim angle exceeds  $20^\circ$ . At a small trim angle ( $\theta \leq 20^\circ$ ), passengers are congested at the exit as shown in Fig. 16, because the speed has a relatively little influence and the flow rates at the exit are high in these cases. However, when the trim angle further increases, the flow rate begins to decrease significantly, and the fluctuation of the flow rate becomes larger with increasing evacuation time. This may be due to the slower speed of pedestrians at a large trim angle, which makes it difficult to evacuate from the room safely, and the flow rate has no continuity and directly results in the average flow rate decrease to 0.90 and 0.25 persons/s at  $\theta = 25^\circ$  and  $\theta = 30^\circ$  respectively. Therefore, it is evident that speed is a key factor affecting the flow rate, and concluded that the best evacuation time window is available when trim angle is smaller than  $20^\circ$  in this scenario.

The above results are based only on a single inclined room, but these can be extended to simulate a deck or full-size ship. Furthermore, the

results can be directly used in some evacuation software when studying evacuation on an inclined plane.

## 5.2. Combination of inclination and density

On cruise ships, it is easy for passengers to gather in restaurants or other public places of entertainment, and the density of passengers tends to be higher in one place than the other. It is helpful to study the evacuation process in places with high passenger density, to understand the characteristics of evacuation in these places and to reduce the consequence in an emergency evacuation. To study the relationship between the density and evacuation, the exit width  $D = 1$  m, the inclination angle  $\theta = 0^\circ$ , and the room size  $15 \text{ m} \times 15 \text{ m}$  are used in the simulation. The results of 100 simulations for  $N = 50$  to 300 with 50 people are shown in Fig. 18. According to the results, the more pedestrians there are in the room, the longer the evacuation time is, and the larger the distribution span of the evacuation time. When  $N = 50$ , the average evacuation time is 25.0 s, the time distribution ranges from 19.4 s to 33.9 s, and the time span is 14.5 s. With the increase in the number of evacuees, the time distribution ranges gradually increase. However, when  $N = 250$ , the maximum evacuation time reaches 132.4 s, and the minimum is 95.4 s. The span of the time distribution range reaches the largest (37.1 s). It is 0.8 s longer than the span of 36.3 s of the time distribution, which ranges from 128.7 s to 165.0 s when  $N = 300$ . As shown in Fig. 18 (b), for the flow rate at the exit, it can be observed that when  $N = 100$ , the average flow rate reaches a maximum of 2.01 persons/s. The flow rate decreases with the increase of the number of pedestrians in room when  $N > 100$ . The finding reveals that 1) the number of conflicts may increase with the increasing number of evacuees in the evacuation process; and 2) individuals need to speed up to reduce their hesitation time to deal with conflicts, thus reducing the total evacuation time (Zou et al., 2020).

Moreover, with increasing trim angles, the overall change trend of the time for different numbers of evacuees is consistent. As shown in Fig. 19, in the change curve of the same number of evacuees, the total evacuation time starts to increase sharply after the trim angle exceeds  $20^\circ$ . When the trim angle is less than  $20^\circ$ , the increase range of evacuation time is 16.9–31.3 s for every 50 people added to the room, and the evacuation time increased by 25.8 s on average. When the trim angle exceeds  $20^\circ$ , the trend of the total evacuation time for different people is similar to that in Fig. 15 and the changes start following an exponential distribution. Therefore, it is found that the number of passengers is the key factor influencing evacuation when  $\theta \leq 20^\circ$  in Fig. 18, while when  $\theta > 20^\circ$ , both the population and inclination have a significant impact on evacuation.

In a real emergency evacuation, especially in the case of serious inclination, not only the deceleration of passengers should be considered, but also the crew should provide guides and lead the process of evacuation in a good order (Fang et al., 2021). As the results shown, if ship capsizing is inevitable in an emergency, the crew should inform the passengers to abandon the ship as early as possible, and evacuate passengers before the inclination angle is  $>20^\circ$ . After this effective time window, the evacuation time could be significantly prolonged. When evacuation has to be carried out under large angles of inclination, both the heeling and trim greatly hinder evacuation. Compared with the impact of heeling on the evacuation process, the influence of trim on walking speed attenuation is less. However, it is still revealed that pedestrians should use fixed devices such as handrails to maintain their balance in all cases of trim and heeling to avoid falling down and injury. In addition, considering that the crew members are familiar with the ship layout, their intervention can effectively avoid the delay of evacuation. Therefore, the crew can play a leading role and provide guide and support to the orderly evacuation. In congested areas, the crew should conduct on-site command, through effective arrangements to speed up pedestrian passage. Alleviating congestion at exits or other areas can greatly improve the evacuation efficiency.

## 6. Conclusions

To investigate the effect of an inclined ship on pedestrian movement, an improved SFMS model is constructed in this paper by adding the inclined force and subjective self-adjusting force to the basic SFM. Simultaneously, to study the attenuation law of the speed more accurately, the dynamic angle  $\lambda$  between the moving direction and the inclination one is introduced, and the influence of the walking direction on speed attenuation is calculated for each time step. At the same time, to avoid pedestrians getting stuck, appropriate random forces are selected.

It is found that speed is not the only factor affecting evacuation. At the same inclination, the influence of heeling on an individual's walking speed is slightly greater than that of trim. The walking direction of pedestrians may also affect the evacuation process. Although the pedestrian speed may decrease to a certain extent in the range of  $10^\circ < \theta < 20^\circ$ , the overall evacuation time does not change much, which indicates that the impact of the inclination angle on pedestrians is still controllable. It can be reasonably concluded that  $\theta \leq 20^\circ$  reflects the best condition for evacuation. It is recommended that the crew should undertake evacuation as soon as possible to avoid trim or heeling angles exceeding  $20^\circ$ . When  $\theta > 20^\circ$ , the pedestrian speed reduces rapidly, which directly leads to a sharp increase in evacuation time. Through the analysis of the evacuation process, it can be observed that pedestrians always generate a large area of congestion at exits, which results in long waiting time. It is also found that the larger the inclination angle is, the more serious congestion and the lower the flow rate at exits. Furthermore, the “fast-is-slow” phenomenon is observed when there is no inclination due to the high speed at which pedestrians gather at exits, resulting in congestion, which in turn reduces the flow rate of evacuees at exits.

In addition, the effect of different evacuation densities on the evacuation time is analysed, and it is found that the increase range of evacuation time is 16.9–31.3 s for every 50 more evacuees in room. The flow rate reaches the maximum when the number of evacuees in the room is 100, and the evacuation efficiency is arriving at the highest level. Through the comprehensive analysis of the impact of inclination and density, the evacuation time is mainly affected by the number of evacuees when  $\theta \leq 20^\circ$ . Conversely, when the inclination angle exceeds  $20^\circ$ , the evacuation time of any scenarios with a different number of people increases significantly.

The new findings can be used as input parameters to simulate more complex scenarios by evacuation software, which provide useful insights on crowd management when ships encounter emergency evacuation. Because of the experimental setting, there are some limitations in this research. Firstly, only an open public area/room on a ship is simulated and analysed in the experiments, which involves little barrier concern. Secondly, ship motion and the heterogeneous behaviours of evacuees in emergency are to be further investigated. Finally, the model and results can only fit the ship accident scenarios involving fixed inclination (e.g., grounding), the inclination angle change with time in capsizing should be investigated further. These limitations should and will be addressed in future.

## CRedit authorship contribution statement

**Siming Fang:** Conceptualization, Writing - original draft, Methodology, Software. **Zhengjiang Liu:** Formal analysis, Supervision. **Xinjian Wang:** Funding acquisition, Investigation, Project administration. **Jin Wang:** Validation, Writing - review & editing. **Zaili Yang:** Data curation, Writing - review & editing, Visualization, Resources.

## Declaration of Competing Interest

The authors declare that they have no known competing financial interests or personal relationships that could have appeared to influence the work reported in this paper.

## Acknowledgements

This work was supported by the National Science Foundation of

China (grant No. 52101399 and 52171353).

## Appendix A. Results of random force tests

The random force was tested in 7 types of forces: random,  $f_{will}$ ,  $1/2 f_{will}$ ,  $1/3 f_{will}$ ,  $1/4 f_{will}$ ,  $1/3 f_{wall}$ , and  $1/3 f_{ij}$ . The times of penetrating boundaries and at an impasse and mean displacement are the evaluation indexes of test. The objective of these tests is to select a random force that can help the pedestrian out of the impasse and avoid penetrating boundaries while keeping the displacement as short as possible. Furthermore, in order to enlarge the difference, the time step was set to 0.5 s. The results are shown in Table 1.

## Appendix B. Detailed fitting data and functions

See Table 2.

Detailed Eq. (9) and (10):

$$\sigma(\theta) = 0.21 \times \exp\left(-\left(\frac{\theta - 20.23}{4.87}\right)^2\right) + 1.05 \times \exp\left(-\left(\frac{\theta + 5.01}{16.14}\right)^2\right) + 0.56 \times \exp\left(-\left(\frac{\theta - 15.18}{10.62}\right)^2\right) + 0.40 \times \exp\left(-\left(\frac{\theta + 20.56}{6.16}\right)^2\right)$$

$$\sigma(\theta_{\perp}) = 96.43 \times \exp\left(-\left(\frac{\theta_{\perp} - 7.45}{8.70}\right)^2\right) - 95.52 \times \exp\left(-\left(\frac{\theta_{\perp} - 7.46}{8.64}\right)^2\right) + 0.28 \times \exp\left(-\left(\frac{\theta_{\perp} - 24.08}{5.33}\right)^2\right) + 1.55 \times 10^5 \times \exp\left(-\left(\frac{\theta_{\perp} + 37.08}{9.80}\right)^2\right)$$

## References

- Anvari, B., Bell, M.G.H., Sivakumar, A., Ochieng, W.Y., 2015. Modelling shared space users via rule-based social force model. *Transp. Res. Part C: Emerging Technol.* 51, 83–103. <https://doi.org/10.1016/j.trc.2014.10.012>.
- Bao, Y.u., Huo, F., 2021. An agent-based model for staircase evacuation considering agent's rotational behavior. *Phys. A* 572, 125923. <https://doi.org/10.1016/j.physa.2021.125923>.
- Bartolucci, A., Casareale, C., Drury, J., 2021. Cooperative and competitive behaviour among passengers during the costa concordia disaster. *Saf. Sci.* 134, 105055. <https://doi.org/10.1016/j.ssci.2020.105055>.
- Bles, W., Nooy, S., Boer, L.C., 2001. Influence of ship listing and ship motion on walking speed. *Conference on Pedestrian and Evacuation Dynamics (PED 2001)*. Springer, p. 437.
- Blue, V.J., Adler, J.L., 1998. Emergent fundamental pedestrian flows from cellular automata microsimulation. *Transp. Res. Rec.* 1644 (1), 29–36. <https://doi.org/10.3141/1644-04>.
- Brumley, A., Koss, L.J.P.o.A., 1998. The implication of human behavior on the evacuation of ferries and cruise ships. *Proceedings of AME* 98.
- Clark, A.G., Walkinshaw, N., Hierons, R.M., 2021. Test case generation for agent-based models: A systematic literature review. *Inf. Softw. Technol.* 135, 106567. <https://doi.org/10.1016/j.infsof.2021.106567>.
- CNIS, 1988. Human dimension of Chinese adults., Beijing.
- Dias, C., Nishiuchi, H., Hyoudo, S., Todoroki, T., 2018. Simulating Interactions between Pedestrians, Segway Riders and Cyclists in Shared Spaces Using Social Force Model. *Transp. Res. Procedia* 34, 91–98. <https://doi.org/10.1016/j.trpro.2018.11.018>.
- Fang, S., Liu, Z., Feng, S., Wang, X., 2021. Numerical analysis of influence of ship listing on evacuation efficiency of different pedestrian flows. *J. Transp. Syst. Eng. Inform. Technol.* 21 (1), 201–206.
- Glen, I., 2004. BMT fleet technology: Conference documentation.
- Ha, S., Ku, N.-K., Roh, M.-I., Lee, K.-Y., 2012. Cell-based evacuation simulation considering human behavior in a passenger ship. *Ocean Eng.* 53, 138–152. <https://doi.org/10.1016/j.oceaneng.2012.05.019>.
- Helbing, D., Farkas, I., Vicsek, T., 2000. Simulating dynamical features of escape panic. *Nature* 407 (6803), 487–490. <https://doi.org/10.1038/35035023>.
- Helbing, D., Molnár, P., 1995. Social force model for pedestrian dynamics. *Phys. Rev. E* 51 (5), 4282–4286.
- Huang, D.Z., Hua, Y.M., Loughney, S., Blanco-Davis, E., Wang, J., 2021. Lifespan cost analysis of alternatives to global sulphur emission limit with uncertainties. *Proc. IME M J. Eng. Marit. Environ.* 235 (4), 921–930. <https://doi.org/10.1177/1475090220983140>.
- Hwang, Y., Heo, G., 2021. Development of a radiological emergency evacuation model using agent-based modeling. *Nucl. Eng. Technol.* 53 (7), 2195–2206. <https://doi.org/10.1016/j.net.2021.01.007>.
- IMO, 2016. Revised Guidelines for Evacuation Analysis for New and Existing Passenger Ships. *MSC.1/Circ* 1533.
- Johansson, F., Peterson, A., Tapani, A., 2015. Waiting pedestrians in the social force model. *Phys. A* 419, 95–107. <https://doi.org/10.1016/j.physa.2014.10.003>.
- Kang, Z., Zhang, L., Li, K., 2019. An improved social force model for pedestrian dynamics in shipwrecks. *Appl. Math. Comput.* 348, 355–362. <https://doi.org/10.1016/j.amc.2018.12.001>.
- Katsuhara, M., Okazaki, T., Kameyama, M., Miyata, O., 1999. Simulation of human escape on board considering human factor. *J.-Japan Soc. Saf. Eng.* 38, 443–449.
- Katuhara, M., Kameyama, M., Miyata, O., Takasugi, Y., Sakane, Y., 1997. Simulation of human escape on board-I. *J. Japan Inst. Navigation* 96 (0), 283–293.
- Kim, H., Haugen, S., Utne, I.B., 2016. Assessment of accident theories for major accidents focusing on the MV SEWOL disaster: Similarities, differences, and discussion for a combined approach. *Saf. Sci.* 82, 410–420. <https://doi.org/10.1016/j.ssci.2015.10.009>.
- Kim, H., Park, J.-H., Lee, D., Yang, Y.-S., 2004. Establishing the methodologies for human evacuation simulation in marine accidents. *Comput. Ind. Eng.* 46 (4), 725–740. <https://doi.org/10.1016/j.cie.2004.05.017>.
- Kim, H., Roh, M.-I., Han, S., 2019. Passenger evacuation simulation considering the heeling angle change during sinking. *Int. J. Nav. Archit. Ocean Eng.* 11 (1), 329–343. <https://doi.org/10.1016/j.ijnaoe.2018.06.007>.
- Lee, D., Park, J.-H., Kim, H., 2004. A study on experiment of human behavior for evacuation simulation. *Ocean Eng.* 31 (8–9), 931–941. <https://doi.org/10.1016/j.oceaneng.2003.12.003>.
- Li, J., Chen, M., Wu, W., Liu, B., Zheng, X., 2021. Height map-based social force model for stairway evacuation. *Saf. Sci.* 133, 105027. <https://doi.org/10.1016/j.ssci.2020.105027>.
- Liang, M., Xu, J., Jia, L., Qin, Y., 2020. An improved model of passenger merging in a Y-shaped passage. *Phys. A* 540, 123233. <https://doi.org/10.1016/j.physa.2019.123233>.
- Liu, B., Liu, H., Zhang, H., Qin, X., 2018. A social force evacuation model driven by video data. *Simul. Model. Pract. Theory* 84, 190–203. <https://doi.org/10.1016/j.simpat.2018.02.007>.
- Lovreglio, R., Kinatered, M., 2020. Augmented reality for pedestrian evacuation research: Promises and limitations. *Saf. Sci.* 128, 104750. <https://doi.org/10.1016/j.ssci.2020.104750>.
- Lovreglio, R., Spearpoint, M., Girault, M., 2019. The impact of sampling methods on evacuation model convergence and egress time. *Reliab. Eng. Syst. Saf.* 185, 24–34. <https://doi.org/10.1016/j.res.2018.12.015>.
- Ma, L., Chen, B., Wang, X., Zhu, Z., Wang, R., Qiu, X., 2019. The analysis on the desired speed in social force model using a data driven approach. *Phys. A* 525, 894–911. <https://doi.org/10.1016/j.physa.2019.03.087>.
- Ma, Y., Lee, E.W.M., Shi, M., 2017. Dual effects of guide-based guidance on pedestrian evacuation. *Phys. Lett. A* 381 (22), 1837–1844. <https://doi.org/10.1016/j.physleta.2017.03.050>.
- Ma, Y., Yuen, R.K.K., Lee, E.W.M., 2016. Effective leadership for crowd evacuation. *Phys. A* 450, 333–341. <https://doi.org/10.1016/j.physa.2015.12.103>.
- Murayama, M., Itagaki, T., Yoshida, K., 2000. Study on evaluation of escape route by evacuation simulation escape in listed ship. *J. Soc. Naval Architects of Japan* 2000 (188), 441–448.

- Ni, B.C., Li, Z., Li, X., 2017. Agent-based evacuation in passenger ships using a goal-driven decision-making model. *Polish Maritime Research* 24 (2), 56–67. <https://doi.org/10.1515/pomr-2017-0050>.
- Park, K.-P., Ham, S.-H., Ha, S., 2015. Validation of advanced evacuation analysis on passenger ships using experimental scenario and data of full-scale evacuation. *Comput. Ind.* 71, 103–115. <https://doi.org/10.1016/j.compind.2015.03.009>.
- Ruggiero, L., Charitha, D., Xiang, S., Lucia, B., 2018. Investigating pedestrian navigation in indoor open space environments using big data. *Appl. Math. Model.* 62, 499–509. <https://doi.org/10.1016/j.apm.2018.06.014>.
- Song, X.B., Lovreglio, R., 2021. Investigating personalized exit choice behavior in fire accidents using the hierarchical Bayes estimator of the random coefficient logit model. *Analytic Methods in Accident Research* 29, 100140. <https://doi.org/10.1016/j.amar.2020.100140>.
- Sticco, I.M., Frank, G.A., Dorso, C.O., 2020. Effects of the body force on the pedestrian and the evacuation dynamics. *Saf. Sci.* 129, 104829. <https://doi.org/10.1016/j.ssci.2020.104829>.
- Sticco, I.M., Frank, G.A., Dorso, C.O., 2021. Social Force Model parameter testing and optimization using a high stress real-life situation. *Phys. A* 561, 125299. <https://doi.org/10.1016/j.physa.2020.125299>.
- Sun, J., Guo, Y., Li, C., Lo, S., Lu, S., 2018a. An experimental study on individual walking speed during ship evacuation with the combined effect of heeling and trim. *Ocean Eng.* 166, 396–403. <https://doi.org/10.1016/j.oceaneng.2017.10.008>.
- Sun, J., Lu, S., Lo, S., Ma, J., Xie, Q., 2018b. Moving characteristics of single file passengers considering the effect of ship trim and heeling. *Phys. A* 490, 476–487. <https://doi.org/10.1016/j.physa.2017.08.031>.
- Valanto, P., 2006. Time-dependent Survival Probability of a Damaged Passenger Ship in evacuation in Seaway and Capsizing. HSVA Report (1661).
- Wang, H., Liu, Z., Wang, X., Graham, T., Wang, J., 2021a. An analysis of factors affecting the severity of marine accidents. *Reliab. Eng. Syst. Saf.* 210, 107513. <https://doi.org/10.1016/j.res.2021.107513>.
- Wang, X., Liu, Z., Wang, J., Loughney, S., Yang, Z., Gao, X., 2021b. Experimental study on individual walking speed during emergency evacuation with the influence of ship motion. *Phys. A* 562, 125369. <https://doi.org/10.1016/j.physa.2020.125369>.
- Wang, X., Liu, Z., Wang, J., Loughney, S., Zhao, Z., Cao, L., 2021c. Passengers' safety awareness and perception of wayfinding tools in a Ro-Ro passenger ship during an emergency evacuation. *Saf. Sci.* 137, 105189. <https://doi.org/10.1016/j.ssci.2021.105189>.
- Wang, X., Liu, Z., Zhao, Z., Wang, J., Loughney, S., Wang, H., 2020. Passengers' likely behaviour based on demographic difference during an emergency evacuation in a Ro-Ro passenger ship. *Saf. Sci.* 129, 104803. <https://doi.org/10.1016/j.ssci.2020.104803>.
- Weidmann, U., 1993. *Transporttechnik der Fußgänger: transporttechnische eigenschaften des fußgängerverkehrs, literaturauswertung*. Weidmann, Ulrich, p. 90.
- Xie, Q., Li, S., Ma, C., Wang, J., Liu, J., Wang, Y., 2020a. Uncertainty analysis of passenger evacuation time for ships' safe return to port in fires using polynomial chaos expansion with Gauss quadrature. *Appl. Ocean Res.* 101, 102190. <https://doi.org/10.1016/j.apor.2020.102190>.
- Xie, Q., Wang, P., Li, S., Wang, J., Lo, S., Wang, W., 2020b. An uncertainty analysis method for passenger travel time under ship fires: A coupling technique of nested sampling and polynomial chaos expansion method. *Ocean Eng.* 195, 106604. <https://doi.org/10.1016/j.oceaneng.2019.106604>.
- Xie, Q., Zhang, S., Wang, J., Lo, S., Guo, S., Wang, T., 2020c. A surrogate-based optimization method for the issuance of passenger evacuation orders under ship fires. *Ocean Eng.* 209, 107456. <https://doi.org/10.1016/j.oceaneng.2020.107456>.
- Yoshida, K., Murayama, M., Itakaki, T., 2001. Study on evaluation of escape route in passenger ships by evacuation simulation and full-scale trials. *Research Institute of Marine Engineering, Japan*.
- Zhang, H., Liu, H., Qin, X., Liu, B., 2018. Modified two-layer social force model for emergency earthquake evacuation. *Phys. A* 492, 1107–1119. <https://doi.org/10.1016/j.physa.2017.11.041>.
- Zou, B., Lu, C., Mao, S., Li, Y., 2020. Effect of pedestrian judgement on evacuation efficiency considering hesitation. *Phys. A* 547, 122943. <https://doi.org/10.1016/j.physa.2019.122943>.